ACS Medicinal Chemistry Letters

LETTER

pubs.acs.org/acsmedchemlett

Pyrazolopyridine Inhibitors of B-Raf^{V600E}. Part 1: The Development of Selective, Orally Bioavailable, and Efficacious Inhibitors

Steve Wenglowsky,*[,†] Li Ren,[†] Kateri A. Ahrendt,[†] Ellen R. Laird,[†] Ignacio Aliagas,[‡] Bruno Alicke,[‡] Alex J. Buckmelter,[†] Edna F. Choo,[‡] Victoria Dinkel,[†] Bainian Feng,[‡] Susan L. Gloor,[†] Stephen E. Gould,[‡] Stefan Gross,[†] Janet Gunzner-Toste,[‡] Joshua D. Hansen,[†] Georgia Hatzivassiliou,[‡] Bonnie Liu,[‡] Kim Malesky,[‡] Simon Mathieu,[‡] Brad Newhouse,[†] Nicholas J. Raddatz,[†] Yingqing Ran,[‡] Sumeet Rana,[†] Nikole Randolph,[†] Tyler Risom,[†] Joachim Rudolph,[‡] Scott Savage,[‡] LeAnn T. Selby,[†] Michael Shrag,[†] Kyung Song,[‡] Hillary L. Sturgis,[†] Walter C. Voegtli,[†] Zhaoyang Wen,[‡] Brandon S. Willis,[†] Richard D. Woessner,[†] Wen-I Wu,[†] Wendy B. Young,[‡] and Jonas Grina[†]

[†]Array BioPharma, 3200 Walnut Street, Boulder, Colorado 80301, United States

[‡]Genentech, Inc., 1 DNA Way, South San Francisco, California 94080-4990, United States

Supporting Information

ABSTRACT: The V600E mutation of B-Raf kinase results in constitutive activation of the MAPK signaling pathway and is present in approximately 7% of all cancers. Using structure-based design, a novel series of pyrazolopyridine inhibitors of B-Raf^{V600E} was developed. Optimization led to the identification of 3-methoxy pyrazolopyridines **17** and **19**, potent, selective, and orally bioavailable agents that inhibited tumor growth in a mouse xenograft model driven by B-Raf^{V600E} with no effect on body weight. On the basis of their in vivo efficacy and preliminary safety profiles, **17** and **19** were selected for further preclinical evaluation.

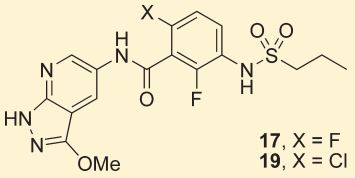

17, X = F
19, X = Cl

KEYWORDS: B-Raf^{V600E}, MAPK pathway, targeted therapy, pyrazolopyridine, amorphous spray-dried dispersion

The Ras/Raf/MEK/ERK (MAPK) signaling pathway transduces signals from cell surface receptors to the nucleus leading to cellular proliferation, differentiation, and survival.[1] The Raf family consists of serine/threonine kinases A-Raf, B-Raf, and C-Raf (Raf-1), which phosphorylate and activate MEK, although with different biochemical potencies (B-Raf > C-Raf ≫ A-Raf).[1] Mutations in the *BRAF* gene may lead to MAPK pathway amplification via constitutive activation of B-Raf kinase and are present in approximately 7% of all cancers.[2] Mutated B-Raf is most frequently associated with melanoma and has been detected in up to 82% of cutaneous melanocyte nevi,[3] 66% of primary melanomas,[2] and 40−68% of metastatic melanomas.[4,5] Additional cancers with aberrant activation of B-Raf due to oncogenic mutations include papillary thryroid cancer (29−83%),[2,6,7] colorectal cancer (5−22%),[2] cholangiocarcinoma (22%),[8] and ovarian cancer (30%).[2] Over 90% of the detected mutations in B-Raf are a glutamic acid for valine substitution at residue 600 (V600E),[2] which leads to constitutive kinase activity 500-fold greater than B-Raf^{WT} and correlates with increased malignancy and decreased response to chemotherapy.[9−12] Thus, cancers induced via constitutive activation of the MAPK signaling pathway arising from B-Raf^{V600E} should be treatable by a small molecule inhibitor targeted to disable this aberrant enzyme.[13] Herein is described the discovery of selective, orally bioavailable, and efficacious inhibitors of B-Raf^{V600E} that utilize a novel 3-methoxy pyrazolopyridine hinge-binding template.

The targeted approach to cancer therapy development has been validated by the growing number of marketed small-molecule protein kinase inhibitors.[14] Although there are no approved kinase inhibitors that are selective for B-Raf^{V600E}, four are currently in clinical trials including RAF265 (Chiron/Novartis),[15] XL281/BMS-908662 (Exelixis/BMS),[16] GSK2118436 (GlaxoSmithKline),[17] and PLX4032 (**1**, Plexxikon/Roche),[18] with others in preclinical development.[19−22] A detailed account of the discovery and clinical development of **1**, a selective B-Raf^{V600E} inhibitor that binds to the active conformation of the kinase (DFG-in), has recently been published.[23] The authors report that the propyl group of the sulfonamide effects B-Raf^{V600E} selectivity by trapping a small lipophilic pocket enlarged by an outward shift of the αC-helix.[24] It was further reported that the difluorophenyl ring of **1** occupies a hydrophobic pocket adjacent to the gatekeeper residue, Thr529.

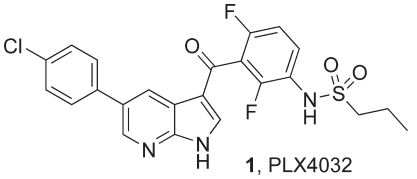

1, PLX4032

From structural evaluation and molecular modeling, it was hypothesized that an amide linker could couple an aryl group in this hydrophobic pocket to a hinge-binding heterocycle, while

Received: November 17, 2010
Accepted: February 26, 2011
Published: March 08, 2011

Scheme 1. Preparation of Pyridine Amides 3−5[a]

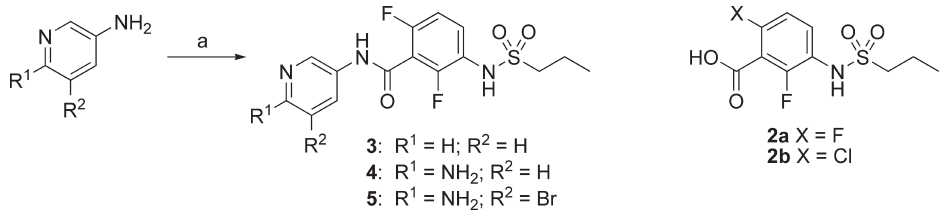

[a] Reagents and conditions: (a) Compound **2a**, EDCI, HOBt, DMF, 22 °C, 5−36%.

Table 1. Enzymatic and Cellular Activities of B-Raf^{V600E} Amide Series Inhibitors

	IC$_{50}$ (nM)		
compd	enzyme[a]	Malme-3M[b]	A375[b]
3	3900	6700	>3000
4	920	2400	>3000
5	110	310	1200
8	61	2400	>3000
9	38	94	290
10	3.4	39	190
13	17	62	430
14	4.0	44	260
15	12	86	830
16	8.2	40	650
17	4.8	19	150
18	6.3	56	560
19	1.7	20	240
1	31[c]	61	190

[a] Biochemical assay (B-Raf^{V600E}). [b] Cellular phosphorylation assay (pERK) using B-Raf^{V600E} mutant Malme-3M or A375 cell line. [c] Ref 23.

forming a hydrogen bond to the hydroxyl of Thr529. Linkage via an amide bond would also allow for rapid and efficient screening of several potential hinge-binding groups. The initial series of amide-linked B-Raf^{V600E} inhibitors utilized pyridine as a hydrogen bond acceptor, which was postulated to bind to the −NH of hinge residue Cys532. Scheme 1 illustrates the synthesis of pyridine-amides **3**−**5** and the structures of the two benzoic acid coupling partners used in this report (**2a** and **2b**).[25]

Inhibitor enzymatic activity was determined utilizing full-length B-Raf^{V600E}. Inhibition of basal ERK phosphorylation in Malme-3M cells was used as the mechanistic cellular assay and to drive the structure−activity relationships for the amide series.[26] Inhibition of ERK phosphorylation was also determined in the A375 cell line and, while up to an order of magnitude less sensitive than the Malme-3M cell line, generated an identical SAR.

The micromolar enzymatic and cellular activity of pyridine amide **3** revealed that additional interactions would be necessary to achieve useful potency (Table 1). Molecular modeling indicated that the addition of a 6-amino group to the pyridine of **3** could yield a hydrogen bond to the carbonyl of Cys532. The 4-fold improvement in enzymatic activity and nearly 3-fold improvement in cellular activity of aminopyridine **4** substantiated this approach. Addition of bromine at the 5-position of **4** led to compound **5** and a further 8-fold increase in enzymatic and cellular activity. The presumed binding model, with hydrogen bonds to Cys532 and Thr529, was confirmed by an X-ray crystal

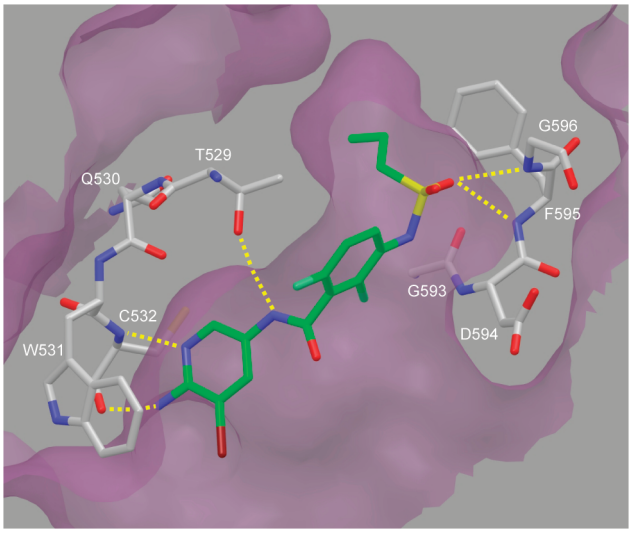

Figure 1. X-ray crystal structure of **5** in complex with B-Raf^{WT}. The cleft surface is rendered in violet, select residues are depicted in white, and the inhibitor is green. Hydrogen-bonding interactions are illustrated with yellow dashed lines. Several residues that are involved in hydrophobic interactions with **5** are omitted for clarity and described in the text. The propyl group resides in a pocket that is enlarged by an outward shift of the αC-helix. The DFG sequence (D594-G596) resides in its active (DFG-in) conformation.

structure of amide **5** with B-Raf (Figure 1). The crystal structure also revealed key lipophilic contacts made by the 5-bromo group with the side chains of Ile463, Val471, Trp531, and Phe583, which accounted for the potency increase over **4**. However, despite the >20-fold improvement in potency from **3** to **5**, the cellular activity of the pyridine amides remained insufficient for in vivo efficacy.

To further improve the potency of the amide series, bicyclic heterocycles were prepared as replacements for the pyridine hinge-binding template. Cyclization of the hinge donor amine of **4** to the 5-position of the pyridine via a five-membered ring suggests three potential bicyclic cores: imidazopyridine, pyrrolopyridine, and pyrazolopyridine. These bicycles were designed to form a bidentate hydrogen-bonding interaction at the hinge, enhance the interaction with the indole of Trp531, and provide a point of diversity for analogue synthesis. Scheme 2 illustrates the synthesis of imidazopyridine and pyrrolopyridine amide series analogues **8**−**10**. Although imidazopyridine **8** had encouraging enzymatic activity, cellular activity was poor (Table 1). This result was surprising given that a related imidazopyrimidine hinge binder has demonstrated excellent cellular activity in an alternative series of B-Raf inhibitors.[22] While pyrrolopyridine **9** had similar enzymatic activity to imidazopyridine **8**, it was 20-fold more active in the cellular assay. In addition, pyrrolopyridine **9** was significantly more

dx.doi.org/10.1021/ml200025q |ACS Med. Chem. Lett. 2011, 2, 342–347

Scheme 2. Preparation of Imidazopyridine and Pyrrolopyridine Amides 8−10[a]

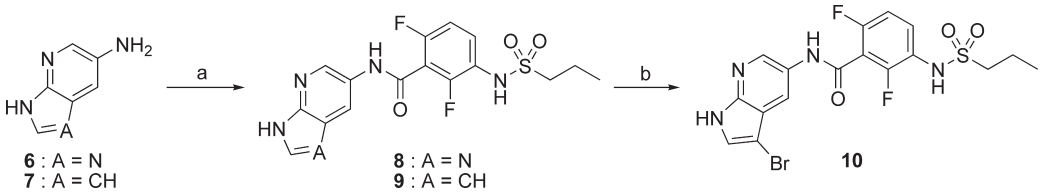

[a] Reagents and conditions: (a) Compound **2a**, EDCI, HOBt, DMF, 22 °C, 9% for **8**, 53% for **9**. (b) Compound **9**, *n*-bromosuccinimide, $CHCl_3$, 82%.

Scheme 3. Preparation of Pyrazolopyridines 13−19[a]

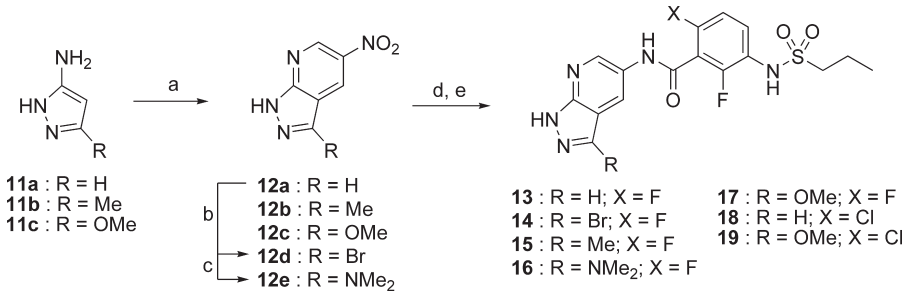

[a] Reagents and conditions: (a) Sodium nitromalonaldehyde monohydrate, AcOH or water, 90 °C, 38−94%. (b) Br_2, NaOH, dioxane, 0−22 °C, 69%. (c) Forty percent $HNMe_2$/water, microwave, 160 °C, 54%. (d) H_2, 10% Pd/C, EtOAc/MeOH, 22 °C, or $SnCl_2$, EtOAc, reflux, 82−99%. (e) Benzoic acid **2a** or **2b**, EDCI, HOBt, DMF, 22 °C, 35−82%.

potent than aminopyridines **4** and **5**, demonstrating the advantage of a bicyclic hinge binder. Bromination at the 3-position of pyrrolopyridine **9** afforded compound **10** and a 2-fold improvement in cellular activity. This result indicated that potency could be increased by an appropriate substitution at the 3-position of the bicyclic hinge-binding template.

The pyrazolopyridine hinge-binding template was prepared concurrently and ultimately provided the most potent B-Raf^{V600E} inhibitors from the amide series. A key advantage of this template included the facility with which substituents of varying electronics could be synthetically incorporated at the 3-position of the core (Scheme 3). Nitromalonaldehyde condensation[27] with 3-substituted-5-aminopyrazoles **11a−c** provided pyrazolopyridines **12a−c**. Bromination of **12a** introduced a synthetic precursor (**12d**) from which a 3-amino pyrazolopyridine (**12e**) was obtained. Nitro reduction of **12a−e** followed by coupling to benzoic acids **2a** or **2b** provided amides **13−19**.

Varying the substituent at the 3-position of the pyrazolopyridine resulted in improvements in the enzymatic and cellular activity of the inhibitors while significantly modulating their pharmacokinetic and physicochemical properties. Unsubstituted pyrazolopyridine **13** was similarly active to the corresponding pyrrolopyridine **9** (Table 1). Most substitutions at the 3-position [Br- (**14**), Me- (**15**), and Me_2N- (**16**)] produced inhibitors within a narrow range of activity and with no significant improvement in potency over **13**. One exception to the flat SAR observed at the 3-position of the pyrazolopyridine template was obtained by the introduction of a methoxy group.[28] This led to 3-methoxy pyrazolopyridine **17**, the most cell potent inhibitor in the amide series. Compounds with halogen substitutions on the benzamide moiety were also examined. While substitution of chloro for fluoro at the 6-position of the benzamide resulted in a 3-fold improvement in the enzymatic activity within two pairs of compounds, there was no change in cellular activity (**18** vs **13** and **19** vs **17**). Compounds **17** and **19** both had similar potency to PLX4032 in the A375 cell line but were 3-fold more potent in Malme-3M cells. The X-ray crystal structure of **17** in complex with B-Raf further confirmed the amide series binding model (Figure 2). Importantly, the proposed interaction of the bicyclic hinge-binding core with Trp531 was validated: A π-stacking interaction between the pyrazole portion of the bicycle and the side chain indole of Trp531 was revealed and likely contributes to the improvement in potency over the pyridine amides **3−5**.[22]

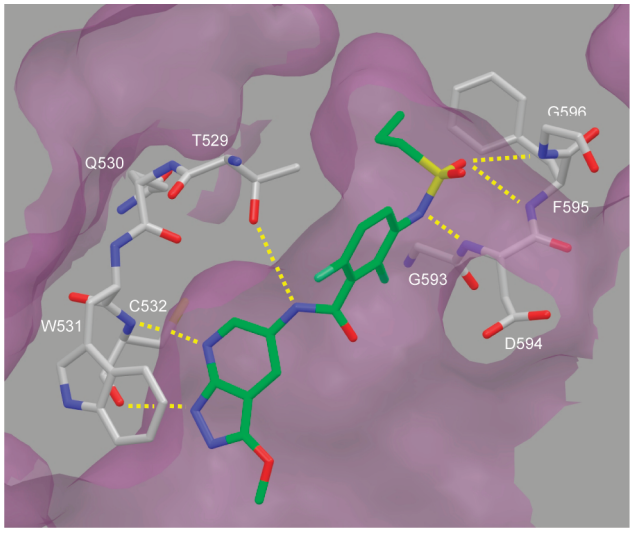

Figure 2. X-ray crystal structure of **17** in complex with B-Raf^{WT}. Notation is as described for Figure 1. In addition to the hydrogen-bonding interactions described in Figure 1, the sulfonamide NH of **17** is in close contact to the main chain NH of Asp594, indicating that the sulfonamide is deprotonated.[23]

dx.doi.org/10.1021/ml200025q |*ACS Med. Chem. Lett.* 2011, 2, 342–347

Table 2. Mouse Pharmacokinetics and Physicochemical Properties of Pyrrolo- and Pyrazolopyridine Amides

compd	30 mg/kg po AUC[a] (% *F*)	100 mg/kg po AUC[a] (% *F*)	CL[b]	Vd[c]	mouse PPB[d]	mp (°C)	sol. at pH 6.5, 7.4[e]
9	200 (76)		1.9	0.20	97.9	243	1, 4
10	49 (71)		7.2	0.24	99.4	227	<1, <1
13	40 (100)		15	0.68	87.1	173	80, 150
14	52.5				98.4	220	1, 3
15	18.3				89.9	181	380, 740
16	1.09				90.8	181	290, 450
17	190 (48)	664 (51)	1.3	0.11	97.4	229	4, 9
18	147 (67)		2.3	0.17	97.1	236	15, 48
19	1080 (53)	50.7 (1.2)	1	0.11	99.1	261	<1, 2

[a] μg h/mL. [b] mL/min/kg. [c] L/kg. [d] Plasma protein binding (%). [e] μg/mL.

Both the nature of the bicyclic template and its substituents were found to have significant effects on the pharmacokinetic and physicochemical properties of the amide series inhibitors (Table 2). Pyrrolo- and pyrazolopyridine amides were dosed orally in mice at 30 mg/kg as a solution in 40% PEG400/10% ethanol/50% water, while select compounds were also dosed intravenously. These compounds typically exhibited high oral bioavailability (% *F*) and oral exposure (AUC). The total clearance (CL) and volume of distribution (Vd) were low and, with the exception of **10**, correlated with plasma protein binding (PPB). Aqueous solubility varied across the series and correlated with melting point (mp), which broadly ranged from 173 to 261 °C; these data suggest that subtle crystal packing effects exist within this series, which could be modulated by varying the substituents around the molecule. Unfortunately, the compounds with the highest aqueous solubilities also exhibited the lowest oral exposures (**13**, **15**, and **16**). The substitution of chloro for fluoro at the 6-position of the benzamide ring had pronounced effects on pharmacokinetic and physicochemical properties: attenuated aqueous solubility, increased PPB, lower IV clearance, and significantly higher oral AUC (**18** vs **13** and **19** vs **17**). Overall, compounds **17** and **19** possessed the best combined potency and exposure from this series, which illustrates the advantage of the 3-methoxy pyrazolopyridine hinge-binding template. However, when these two compounds were dosed orally in mice at 100 mg/kg using the same solution formulation, compound **17** exhibited a dose proportional increase in exposure, while the oral bioavailability of **19** dropped to 1%. The low aqueous solubility and high melting point of this compound likely led to crystallization in the gut preventing absorption.

In an effort to rescue the poor pharmacokinetics of compound **19** at higher doses and because of concerns with daily dosing of high concentrations of PEG400 in potential preclinical toxicology and xenograft studies, **17** and **19** were reformulated as a 25% amorphous spray-dried dispersion (SDD) on hydroxypropyl methylcellulose acetate succinate (HPMCAS) polymer.[29] Bridging pharmacokinetic studies in mice with **17** dosed orally at 2.5, 10, 40, and 80 mg/kg revealed a linear dose response, albeit with oral bioavailabilities lower than with the soluble PEG400-based solution formulation (F = 19−25 vs 48−51%). Nonetheless, exposure exceeded the levels projected to achieve efficacy in mouse models of cancer driven by B-Raf^{V600E}. Compound **19** was also dosed as the SDD formulation in mice at 10, 30, 60, and 100 mg/kg and demonstrated decreasing oral bioavailability with increasing dose (F = 53, 28, 19, and 13%). Although a linear dose response was not achieved, this formulation provided a significant improvement in exposure at 100 mg/kg for **19** (13 vs 1%), higher bioavailability than **17** at 10 mg/kg (53 vs 25%), and likewise exceeded the levels projected to achieve efficacy.

Table 3. Dose-Ranging Tumor Growth Inhibition Studies in Colo205 Mouse Xenografts

compd	no. of days dosed	ED_{50}[a]	ED_{90}[a]	max TGI (%)[b]
17	20	20	80	76
19	17	11	50	95

[a] mg/kg. [b] Tumor growth inhibition as a percent of vehicle control.

To further characterize in vitro potency and in preparation for mouse xenograft studies, inhibition of cellular viability by compound **17** was measured against a panel of 13 melanoma and 10 colon cancer cell lines driven by the B-Raf^{V600E} mutation, and potencies were compared to PLX4032 (**1**). In melanoma, **17** was 2−3-fold more potent than **1** in 8 of the 13 cell lines tested and equivalent in the remaining 5, while in colon cancer, **17** was 2−14-fold more potent than **1** in 9 of 10 cell lines examined. Compound **19** was screened against four of the colon cancer cell lines and was similarly more potent than **1**. For Colo205, in which mouse xenograft studies were run, the EC_{50} values for **17** and **19** were 80 and 70 nM as compared to 240 nM for **1**.

The activity of **17** and **19** was also determined against a diverse panel of kinases and demonstrated similar selectivity profiles with >100-fold selectivity for 223/228 kinases examined. Compounds **17** and **19** displayed no inhibition of cytochrome P450 enzymes at 25 μM, no hERG channel inhibition at 100 μM, and were negative in the Ames test for genotoxicity. On the basis of their in vitro potency and favorable pharmacokinetic properties, 3-methoxy pyrazolopyridines **17** and **19** were selected for dose-ranging tumor growth inhibition studies in the Colo205 mouse xenograft model.

The SDD of **17** and **19** were administered at ascending doses once daily for 17 or 20 days in mice with established Colo205 xenografts (Table 3). Tumor growth inhibition was observed for both compounds with a maximum tumor regression of 76% at 125 mg/kg for **17** and 95% at 100 mg/kg for **19**. Analysis of tumor samples indicated that in vivo efficacy requires sustained inhibition of pERK levels of at least 50% for 6 h.[30] Given that compound **19** was similarly active to **17** in the biochemical assay and in several cellular assays, the superior efficacy of **19** across the entire dose range of the xenograft study was presumably due to its higher exposure. The low volumes of distribution for both compounds (Table 2) did not abate the efficacy of the compounds. Significantly, over the course of the dosing period, no

dx.doi.org/10.1021/ml200025q |*ACS Med. Chem. Lett.* 2011, 2, 342–347

toxicity and no significant alterations in body weight were observed at any dose for either **17** or **19**.

In summary, selective, orally bioavailable, and efficacious inhibitors of B-Raf^{V600E} were developed. These inhibitors were based on a novel 3-methoxy pyrazolopyridine hinge-binding template, which evolved through structure-based design from a simple pyridine lead (**3**). While the activity of **3** was micromolar in both enzymatic and cellular assays, the introduction of a hydrogen bond donor, utilization of a bicyclic hinge-binding template, and addition of lipophilic contacts provided potent pyrrolo- and pyrazolopyridine inhibitors of B-Raf^{V600E}. Optimization at the 3-position ultimately led to 3-methoxy pyrazolopyridines **17** and **19**, which demonstrated a 300-fold improvement in potency over the lead pyridine **3**. Compounds **17** and **19** were highly potent against a broad panel of cancer cell lines driven by B-Raf^{V600E}, particularly those derived from colon cancer, and displayed significant antitumor activity in an in vivo colon cancer model driven by B-Raf^{V600E}. Although **17** and **19** were well tolerated in mice during the xenograft studies, RAF inhibitors have been reported to activate the MAPK pathway in B-Raf^{WT} cells.[19,20,22,31−33] This paradoxical activation has been linked to enhanced proliferation and stimulated tumor growth in vivo, and hyperplasia of normal epithelial cells was observed in mice.[34] Pyrazolopyridine Raf inhibitors likewise activate the MAPK pathway, and the results from these studies will be presented elsewhere.

■ ASSOCIATED CONTENT

Supporting Information. Experimental procedures for the synthesis of **3**−**5**, **8**−**10**, **13**−**19**, kinase selectivity, and cell viability data for **17** and **19** and details of in vitro and in vivo assays. This material is available free of charge via the Internet at http://pubs.acs.org.

■ AUTHOR INFORMATION

Corresponding Author

*Tel: 303-641-1076. E-mail: steve.wenglowsky@arraybiopharma.com.

■ ACKNOWLEDGMENT

We thank Josh Ballard for HRMS data and Ben Colson for solubility determinations. We also thank Jim Blake for helpful discussions.

■ REFERENCES

(1) Peyssonnaux, C.; Eychene, A. The Raf/MEK/ERK pathway: New concepts of activation. *Biol. Cell.* **2001**, *93*, 53–62.

(2) Davies, H.; Bignell, G. R.; Cox, C.; Stephens, P.; Edkins, S.; Clegg, S.; Teague, J.; Woffendin, H.; Garnett, M. J.; Bottomley, W.; Davis, N.; Dicks, E.; Ewing, R.; Floyd, Y.; Gray, K.; Hall, S.; Hawes, R.; Hughes, J.; Kosmidou, V.; Menzies, A.; Mould, C.; Parker, A.; Stevens, C.; Watt, S.; Hooper, S.; Wilson, R.; Jayatilake, H.; Gusterson, B. A.; Cooper, C.; Shipley, J.; Hargrave, D.; Pritchard-Jones, K.; Maitland, N.; Chenevix-Trench, G.; Riggins, G. J.; Bigner, D. D.; Palmieri, G.; Cossu, A.; Flanagan, A.; Nicholson, A.; Ho, J. W. C.; Leung, S. Y.; Yuen, S. T.; Weber, B. L.; Seigler, H. F.; Darrow, T. L.; Paterson, H.; Marais, R.; Marshall, C. J.; Wooster, R.; Stratton, M. R.; Futreal, P. A. Mutations of the BRAF gene in human cancer. *Nature* **2002**, *417*, 949–954.

(3) Pollock., P. M.; Harper, U. L.; Hansen, K. S.; Yudt, L. M.; Stark, M.; Robbins, C. M.; Moses, T. Y.; Hostetter, G.; Wagner, U.; Kakereka, J. Salem, G.; Pohida, T.; Heenean, P.; Duray, P.; Kallioniemi, O.; Hayward, N. K.; Trent, J. M.; Meltzer, P. S. High frequency of B-Raf mutations in nevi. *Nat. Genet.* **2003**, *33*, 19–20.

(4) Gorden, A.; Osman, I.; Gai, W.; He, D.; Huang, W.; Davidson, A.; Houghton, A. N.; Busam, K.; Polsky, D. Analysis of B-Raf and N-Ras mutations in metastatic melanoma tissues. *Cancer Res.* **2003**, *63*, 3955–3957.

(5) Kuman, R.; Angelini, S.; Czene, K.; Sauroja, I.; Hahka-Kemppinen, M. Pyrhonen, S.; Hemminki, K. B-Raf mutations in metastatic melanoma: A possible association with clinical outcome. *Clin. Cancer Res.* **2003**, *9*, 3362–3368.

(6) Riesco-Eizaguirre, G.; Santisteban, P. New insights in thyroid follicular cell biology and its impact in thyroid cancer therapy. *Endocr.-Relat. Cancer* **2007**, *14*, 957–977.

(7) Li, Y.; Nakamura, M.; Kakudo, K. Targeting of the BRAF gene in papillary thyroid carcinoma (Review). *Oncol. Rep.* **2009**, *22*, 671–681.

(8) Tannapfel, A.; Sommerer, F.; Benicke, M.; Katalinic, A.; Uhlmann, D.; Witzigmann, H.; Hauss, J.; Wittekind, C. Mutations of the BRAF gene in cholangiocarcinoma but not in hepatocellular carcinoma. *Gut* **2003**, *52*, 706–712.

(9) Wan, P. T.; Garnett, M. J.; Roe, S. M.; Lee, S.; Niculescu-Duvaz, D.; Good, V. M.; Jones, C. M.; Marshall, C. J.; Springer, C. J.; Barford, D.; Marais, R. Mechanism of activation of the RAF-ERK signaling pathway by oncogenic mutations of B-RAF. *Cell* **2004**, *116*, 855–867.

(10) Samowitz, W. S.; Sweeney, C.; Herrick, J.; Albertsen, H.; Levin, T. R.; Murtaugh, M. A.; Wolff, R. K.; Slattery, M. L. Poor survival associated with the BRAF V600E mutation in microsatellite-stable colon cancers. *Cancer Res.* **2005**, *65*, 6063–6069.

(11) Riesco-Eizaguirre, G.; Gutierrez-Martinez, P.; Garcia-Cabezas, M. A.; Mistal, M.; Santisteban, P. The oncogene BRAF V600E is associated with a high risk of recurrence and less differentiated papillary thyroid carcinoma due to the impairment of Na+/I-targeting to the membrane. *Endocr.-Relat. Cancer* **2006**, *13*, 257–269.

(12) Houben, R.; Becker, J. C.; Kappel, A.; Terheyden, P.; Bröcker, E. B.; Goetz, R.; Rapp, U. R. Constitutive activation of the Ras-Raf signaling pathway in metastatic melanoma is associated with poor prognosis. *J. Carcinog.* **2004**, *3*, 6–18.

(13) Sawyers, C. Targeted cancer therapy. *Nature* **2004**, *432*, 294–297.

(14) Johnson, L. N. Protein kinase inhibitors: Contributions from structure to clinical compounds. *Q. Rev. Biophys.* **2009**, *42*, 1–40.

(15) ClinicalTrials.gov web site. http://www.clinicaltrials.gov (accessed Feb 22, 2011). A study to evaluate RAF265, an oral drug administered to subjects with locally advanced or metastatic melanoma.

(16) Schwartz, G. L.; Robertson, S.; Shen, A.; Wang, E.; Pace, L.; Dials, H.; Mendelson, D.; Shannon, P.; Gordon, M. A phase I study of XL281, a selective oral RAF kinase inhibitor, in patients (Pts) with advanced solid tumors. *J. Clin. Oncol.* **2009**, *27*, 15sAbstr. 3513.

(17) Kefford, R.; Arkenau, H.; Brown, M. P.; Millward, M.; Infante, J. R.; Long, G. V.; Ouellet, D.; Curtis, M.; Lebowitz, P. F.; Falchook, G. S. Phase I/II study of GSK2118436, a selective inhibitor of oncogenic mutant BRAF kinase, in patients with metastatic melanoma and other solid tumors. *J. Clin Oncol.* **2010**, *28*, 15sAbstr. 8503.

(18) Flaherty, K. T.; Puzanov, I.; Kim, K. B.; Ribas, A.; McArthur, G. A.; Sosman, J. A.; O'Dwyer, P. J.; Lee, R. J.; Grippo, J. F.; Nolop, K.; Chapman, P. B. Inhibition of mutated, activated BRAF in metastatic melanoma. *N. Engl. J. Med.* **2010**, *363*, 809–819.

(19) King, A. J.; Patrick, D. R.; Batorsky, R. S.; Ho, M. L; Do, H. T.; Zhang, S. Y.; Kumar, R.; Rusnak, D. W.; Takle, A. K.; Wilson, D. M.; Hugger, E.; Wang, L.; Karreth, F.; Lougheed, J. C.; Lee, J.; Chau, D.; Stout, T. J.; May, E. W.; Rominger, C.; M.; Schaber, M.; D.; Luo, L.; Lakdawala, A. S.; Adams, J. L.; Contractor, R. G.; Smalley, K. S. M.; Herlyn, M.; Morrissey, M. M.; Tuveson, D. A.; Huang, P. S. Demonstration of a Genetic Therapeutic Index for Tumors Expressing Oncogenic BRAF by the Kinase. *Cancer Res.* **2006**, *66*, 11100–11105.

(20) Hoeflich, K. P.; Herter, S.; Tien, J.; Wong, L.; Berru, L.; Chan., J.; O'Brien, C.; Modrusan, Z.; Seshagiri, S.; Lackner, M.; Stern, H.; Choo, E.; Murray, L.; Friedman, L. S.; Belvin, M. Antitumor efficacy of the

novel RAF inhibitor GDC-0879 is predicted by $BRAF^{V600E}$ mutational status and sustained extracellular signal-regulated kinase/mitogen-activated protein kinase pathway suppression. *Cancer Res.* **2009**, *69*, 3042–3051.

(21) Tang, J.; Hamajima, T.; Nakano, M.; Sato, H.; Dickerson, S. H.; Lackey, K. E. Knowledge-based design of 7-azaindoles as selective B-Raf inhibitors. *Bioorg. Med. Chem. Lett.* **2008**, *18*, 4610–4614.

(22) Smith, A. L.; DeMorin, F. F.; Paras, M. A.; Huang, Q.; Petkus, J. K.; Doherty, E. M.; Nixey, T.; Kim, J. L.; Whittington, D. A.; Epstein, L. F.; Lee, M. R.; Rose, M. J.; Babij, C.; Fernando, M.; Hess, K.; Le, Q.; Beltran, P.; Carnahan, J. Selective inhibitors of the mutant B-Raf pathway: Discovery of a potent and orally bioavailable aminoisoquinoline. *J. Med. Chem.* **2009**, *52*, 6289–6292.

(23) Bollag, G.; Hirth, P.; Tsai, J.; Zhang, J.; Ibrahim, P. N.; Cho, H.; Spevak, W.; Zhang, C.; Zhang, Y.; Habets, G.; Burton, E. A.; Wong, B.; Tsang, G.; West., B. L.; Powell, B.; Shellooe, R.; Marimuthu, A.; Nguyen, H.; Zhang, K. Y. J.; Artis, D. R.; Schlessinger, J.; Su, F.; Higgins, B.; Iyer, R.; D'Andrea, K.; Koehler, A.; Stumm, M.; Lin., P. S.; Lee, R. J.; Grippo, J.; Puzanov, I.; Kim, K. B.; Ribas, A.; McArthur, G. A.; Sosman, J. A.; Chapman, P. B.; Flaherty, K. T.; Xu, X.; Nathanson, K. L.; Nolop, K. Clinical efficacy of a RAF inhibitor needs broad target blockade in BRAF-mutant melanoma. *Nature* **2010**, *467*, 596–599.

(24) Via a substituted benzyl ether, lapatinib also traps a shifted αC-helix in EGFR kinase, which similarly leads to high kinase selectivity: Wood, E. R.; Truesdale, A. T.; McDonald, O. B.; Yuan, D.; Hassell, A.; Dickerson, S. H.; Ellis, B.; Pennisi, C.; Horne, E.; Lackey, K.; Alligood, K. J.; Rusnak, D. W.; Gilmer, T. M.; Shewchuk, L. A unique structure for epidermal growth factor receptor bound to GW572016 (lapatinib): Relationships among protein conformation, inhibitor off-rate, and receptor activity in tumor cells. *Cancer Res.* **2004**, *64*, 6652–6659.

(25) Ahrendt, K. A.; Buckmelter, A. J.; De Meese, J.; Grina, J.; Hansen, J. D.; Laird, E. R.; Lunghofer, P.; Moreno, D.; Newhouse, B.; Ren, L.; Seo, J.; Tian, H.; Wenglowsky, S. M.; Feng, B.; Gunzner, J.; Malesky, K.; Mathieu, S.; Rudolph, J.; Wen, Z.; Young, W. B. N-Pyrazolo[3,4-b]pyridinyl benzamide derivatives as Raf inhibitors and their preparation, pharmaceutical compositions and use in the treatment of diseases. WO 2009/111279.

(26) Wallace, E. M.; Lyssikatos, J.; Blake, J. F.; Seo, J.; Yang, H. W.; Yeh, T. C.; Perrier, M.; Jarski, H.; Marsh, V.; Poch, G.; Livingston, M. G.; Otten, J.; Hingorani, G.; Woessner, R.; Lee, P.; Winkler, J.; Koch, K. Potent and selective mitogen-activated protein kinase kinase (MEK) 1,2 inhibitors. 1. 4-(4-bromo2-2fluorophenylamino)-1-methylpyridin-2(1*H*)-ones. *J. Med. Chem.* **2006**, *49*, 441–444.

(27) Lynch, B. M.; Khan, M. A.; Teo, H. C.; Pedrotti, F. Pyrazolo-[3,4-b]pyridines: Syntheses, reactions, and nuclear magnetic resonance spectra. *Can. J. Chem.* **1988**, *66*, 420–428.

(28) Blake, J.; Gunawardana, I. W.; Le Huerou, Y.; Mohr, P. J.; Wallace, E. M.; Wang, B. Pyrazolopyridine derivatives and their pharmaceutical compositions as CHK1 and CHK2 kinase inhibitors for the treatment of various diseases and preparation thereof. WO 2009/089359.

(29) Friesen, D. T.; Shanker, R.; Crew, M.; Smithey, D. T.; Curatolo, W. J.; Nightingale, J. A. S. Hydroxypropyl methylcellulose acetate succinate-based spray-dried dispersions: An overview. *Mol. Pharmaceutics* **2008**, *5*, 1003–1019.

(30) Details and discussion regarding the relationship between pERK inhibition and tumor response will be reported:Choo, E. F.; Afflerbaugh, L.; Alicke, B.; Boggs, J.; Dinkel, D.; Gould, S.; Grina, J.; West, K.; Menghrajani, K.; Ran, Y.; Rudolph, J.; Wenglowsky, S. Preclinical Assessment of Novel B-RAF Inhibitors: Integrating Pharmacokinetic-Pharmacodynamic Modeling in the Drug Discovery Process. *Xenobiotica*, manuscript in preparation.

(31) Hatzivassiliou, G.; Song, K.; Yen, I.; Brandhuber, B. J.; Anderson, D. J.; Alvarado, R.; Ludlam, M. C.; Stokoe, D.; Gloor, S. L.; Vigers, G.; Morales, T.; Aliagas, I.; Liu, B.; Siberis, S.; Hoeflich, K. P.; Jaiswal, B. S.; Seshagiri, S.; Koeppen, H.; Belvin, M.; Friedman, L. S.; Malek, S. RAF inhibitors prime wild-type RAF to activate the MAPK pathway and enhance growth. *Nature* **2010**, *464*, 431–435.

(32) Heidhorn, S. J.; Milagre, C.; Whittaker, S.; Nourry, A.; Niculescu-Duvas, I.; Dhomen, N.; Hussain, J.; Reis-Filho, J.; Springer, C. J.; Pritchard, C.; Marais, R. Kinase-dead BRAF and oncogenic RAS cooperate to drive tumor progression through CRAF. *Cell* **2010**, *140*, 209–221.

(33) Poulikakos, P.; Zhang, C.; Bollag, G.; Shokat, K. M.; Rosen, N. RAF inhibitors transactivate RAF dimers and ERK signaling in cells with wild-type BRAF. *Nature* **2010**, *464*, 427–430.

(34) Carnahan, J.; Beltran, P. J.; Babij, C.; Le, Q.; Rose, M. J.; Vonderfecht, S.; Kim, J. L.; Smith, A. L.; Nagapudi, K.; Broome, M. A.; Fernando, M.; Kha, H.; Belmontes, B.; Radinsky, R.; Kendall, R.; Burgess, T. L. Selective and potent Raf inhibitors paradoxically stimulate normal cell proliferation and tumor growth. *Mol. Cancer Ther.* **2010**, *9*, 2399–2410.